High-temperature thermoelectric properties of $Ca_{0.9-x}Sr_xYb_{0.1}MnO_{3-\delta}$ $(0 \leq x \leq 0.2)$

Atsuko Kosuga,[1,a] Yuri Isse,[2] Yifeng Wang,[3] Kunihito Koumoto,[3,4] and Ryoji Funahashi[1,4]
[1]*National Institute of Advanced Industrial Science and Technology, Ikeda, Osaka 563-8577, Japan*
[2]*Osaka Electro-Communication University, Neyagawa, Osaka 572-0833, Japan*
[3]*Graduate School of Engineering, Nagoya University, Furo-cho, Chikusa, Nagoya 464-8603, Japan*
[4]*CREST, Japan Science and Technology Agency, Kawaguchi, Saitama 332-0012, Japan*

(Received 3 February 2009; accepted 29 March 2009; published online 13 May 2009)

Polycrystalline samples of $Ca_{0.9-x}Sr_xYb_{0.1}MnO_{3-\delta}$ (x=0, 0.025. 0.05, 0.1, and 0.2) were prepared by a conventional solid-state reaction and their thermoelectric properties were evaluated at 303–973 K. Each of the samples consisted of a single phase with an orthorhombic structure. All the samples showed a metallic conductivity and their electrical resistivity was markedly affected by the distortion of the MnO_6 octahedron. The Seebeck coefficient of all the samples was negative, indicating that the predominant carriers were electrons over the entire temperature range examined. The highest power factor achieved (0.22 mW m^{-1} K^{-2} at 773 K) was shown by the sample with x=0.1. The thermal conductivity was affected by both the crystal distortion and the difference in mass between the Ca^{2+} and Sr^{2+} ions. The highest dimensionless figure of merit obtained was 0.09 at 973 K for the sample with x=0.1; this is a result of its low electrical resistivity and its moderate Seebeck coefficient and thermal conductivity. © *2009 American Institute of Physics*. [DOI: 10.1063/1.3125450]

I. INTRODUCTION

Thermoelectric energy conversion can be used to generate electricity from waste heat. The efficiency of thermoelectric materials in this process is determined by their dimensionless thermoelectric figure of merit, $ZT=S^2\sigma T/\kappa$, where S, σ, T, and κ are the Seebeck coefficient, the electrical conductivity, the absolute temperature, and the thermal conductivity, respectively.[1,2] In the past few decades, several innovative bulk intermetallic compounds that exhibit high values of ZT ($\approx$1) have been identified and developed.[3–5] Despite their high ZT value, these compounds are of limited practical use because of their low chemical stability in air at high temperatures. The realization of widespread large-scale industrial use of thermoelectric technology is contingent on the development of thermoelectric bulk materials that have a low cost, are environmentally friendly, and are stable at high temperatures in air. Thermoelectric bulk oxides have attracted considerable attention because they fulfill these requirements. Since the discovery of p-type Na_xCoO_2,[6] which has an unexpectedly high absolute value of S despite possessing metallic conductivity, numerous researchers have made extensive studies on oxide materials. For instance, the p-type Co-based oxides $Ca_3Co_4O_9$ (Co-349) and $Bi_2Sr_2Co_2O_9$ (BC-222) have been shown to exhibit high ZT values at high temperatures in air.[7,8] Likewise, n-type Nb-doped $SrTiO_3$ and $(Zn_{1-x}Al_x)O$ with high ZT values have been developed;[9,10] however, neither Nb-doped $SrTiO_3$ nor $(Zn_{1-x}Al_x)O$ exhibits a high performance in air because both require the presence of a deficiency of oxygen and, additionally, the latter is mechanically too brittle for use in real applications. Thus, n-type oxides with good chemical and mechanical properties are required for power generation.

Calcium manganese perovskites have attracted much attention because they have interesting electrical and magnetic properties[11,12] as a result of their flexible crystal structures. Perovskite compounds have the general formula ABO_3, where A is a rare earth or alkaline earth metal and B is a transition metal, and A and B can be selected from a wide variety of elements. The thermoelectric properties of $CaMnO_3$ doped at A and/or B sites have been widely investigated.[13–17] Among the previously evaluated calcium manganites prepared by a conventional solid-state reaction, the highest ZT value of $\sim$0.2 at 973 K in air was found for $Ca_{0.9}Yb_{0.1}MnO_3$.[14,15] We have developed an oxide module with a $CaMnO_3$ system as an n-type leg,[18] and we succeeded in improving the fracture mechanical properties of $Ca_{0.9}Yb_{0.1}MnO_3$ by incorporating Ag particles,[19] thereby producing a highly reliable thermoelectric module.

In the present study, the effects of partial substitution of Ca sites by Sr on the thermoelectric properties of $Ca_{0.9}Yb_{0.1}MnO_{3-\delta}$ were investigated in an attempt to achieve a further improvement in the thermoelectric performance of the material. Because substitution of Ca sites by Sr changes the A-site volume at a given level of doping, doping by Sr is expected to have a dramatic effect on ρ while retaining a relatively high absolute value of S, leading to the possibility of an enhancement in the thermoelectric properties of the material.

II. EXPERIMENTAL DETAILS

Polycrystalline samples of $Ca_{0.9-x}Sr_xYb_{0.1}MnO_{3-\delta}$ (x=0, 0.025, 0.05, 0.1, and 0.2) were prepared by a conventional solid state reaction. Stoichiometric quantities of high-purity

[a]Electronic mail: kosuga-atsuko@aist.go.jp.

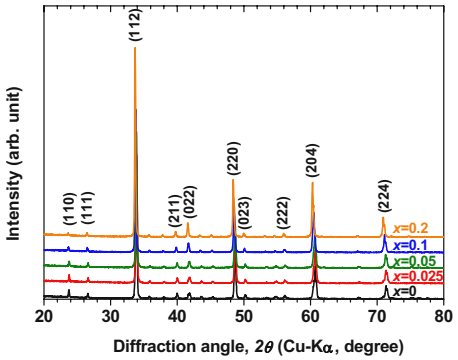

FIG. 1. (Color online) XRD patterns of $Ca_{0.9-x}Sr_xYb_{0.1}MnO_{3-\delta}$ ($x=0$, 0.025, 0.05, 0.1, and 0.2).

$CaCO_3$ (Japan Pure Chemical Co. Ltd.), $SrCO_3$ (Japan Pure Chemical Co. Ltd.), Yb_2O_3 (Shin-etsu Chemical Co. Ltd.), and Mn_2O_3 (Japan Pure Chemical Co. Ltd.) powders were mixed and calcined in air at 1273 K for 15 h to induce decarbonization. The samples were reground and heated at 1523 K for 10 h in air, with an intermediate grinding. Finally, the products were pressed uniaxially into pellets at a pressure of 40 MPa, sintered in air at 1623 K for 15 h, and slowly cooled to room temperature at a rate of approximately 1 K/min. The crystal structure of the samples was analyzed by powder x-ray diffraction (XRD) studies at room temperature using Cu Kα radiation (Rigaku RINT-TTR). The chemical composition of the samples was determined by energy-dispersive x-ray analysis (Horiba EMAX-7000), and their oxygen content was measured with an oxygen analyzer (Horiba EMGA-533). The experimental bulk density d_e of each of the samples was measured by the Archimedes method. The temperature dependence of ρ for the samples was measured in air by a standard dc four-probe method. The thermoelectromotive forces (ΔV) and temperature difference (ΔT) of samples were measured, and S was deduced from the relationship $\Delta V/\Delta T$. Pt–Pt/Rh thermocouples were attached at the two ends of each sample by using silver paste. The Pt wires of the thermocouples were used as voltage terminals. The S values of the Pt wires were subtracted from the measured S values to give the net S values for the samples. The standard deviation of the S was within 2% at all the base temperatures. The values of κ for the samples were calculated from the thermal diffusivity λ, the specific heat capacity C_p, and the density d by applying the following relationship:

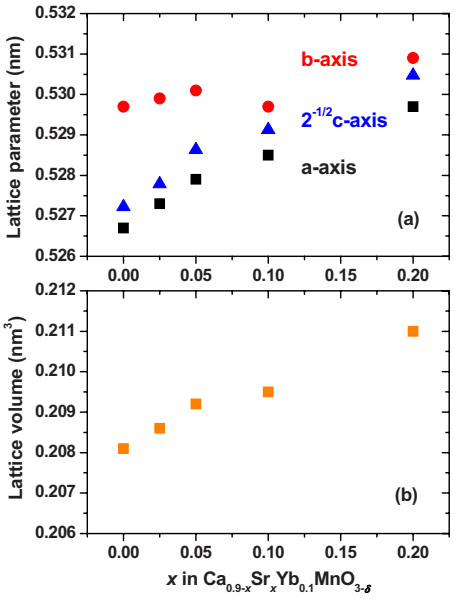

FIG. 2. (Color online) The dependence of (a) the lattice parameters a, b, c and (b) the lattice volume V on the value of x for $Ca_{0.9-x}Sr_xYb_{0.1}MnO_{3-\delta}$ ($x=0$, 0.025, 0.05, 0.1, and 0.2).

$$\kappa = \lambda C_p d. \tag{1}$$

The values of λ and C_p were measured by differential scanning calorimetry (TA Instrument MDSC2910) and the laser-flash method (ULVAC TC3000V) under vacuum, respectively.

III. RESULTS AND DISCUSSION

The XRD patterns at room temperature of the $Ca_{0.9-x}Sr_xYb_{0.1}MnO_{3-\delta}$ ($0 \le x \le 0.2$) samples are shown in Fig. 1. The diffraction peaks of all the samples can be completely indexed as corresponding to an orthorhombic $CaMnO_3$ structure[20] without any measurable impurity phases, indicating that a single phase of orthorhombic $Ca_{0.9-x}Sr_xYb_{0.1}MnO_{3-\delta}$ ($0 \le x \le 0.2$) was obtained in each case. Although we tried to prepare $Ca_{0.9-x}Sr_xYb_{0.1}MnO_{3-\delta}$ ($0 \le x \le 0.9$), a single phase was obtained only for the composition range $x \le 0.45$. Further substitution by Sr for Ca ($x > 0.45$) resulted in the formation of a two-phase mixture of hexagonal α-$SrMnO_{3-\delta}$ (space group $P6_3/mmc$)[21] and orthorhombic $CaMnO_{3-\delta}$ (space group $Pnma$).[20]

Figure 2 shows the dependence of the lattice parameters a, b, and c and the lattice volume V on the level of Sr doping for the $Ca_{0.9-x}Sr_xYb_{0.1}MnO_{3-\delta}$ solid solutions. The values of

TABLE I. Compositions of experimental samples of $Ca_{0.9-x}Sr_xYb_{0.1}MnO_{3-\delta}$ ($x=0$, 0.025, 0.05, 0.1, and 0.2).

	element				
x	Ca	Sr	Yb	Mn	O
0	0.84 ± 0.02	⋯	0.11 ± 0.007	1.00 ± 0.01	2.99 ± 0.03
0.025	0.81 ± 0.05	0.03 ± 0.0087	0.10 ± 0.004	1.01 ± 0.05	2.89 ± 0.04
0.05	0.86 ± 0.02	0.05 ± 0.0084	0.10 ± 0.004	1.00 ± 0.03	2.88 ± 0.02
0.1	0.81 ± 0.01	0.13 ± 0.0093	0.11 ± 0.005	0.98 ± 0.01	2.90 ± 0.01
0.2	0.71 ± 0.02	0.18 ± 0.0110	0.11 ± 0.007	1.00 ± 0.02	2.93 ± 0.01

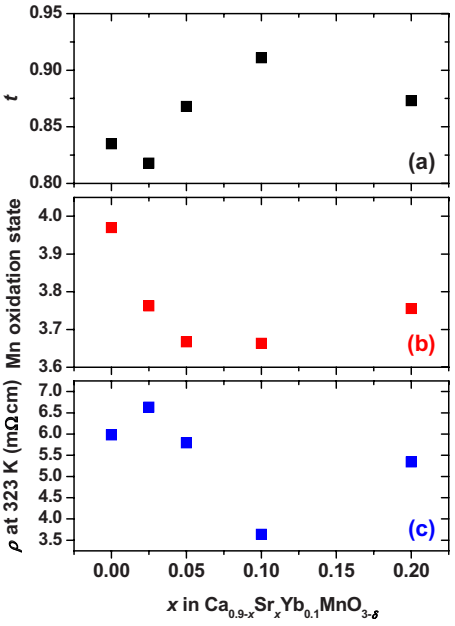

FIG. 3. (Color online) The dependence of (a) tolerance factor t, (b) the Mn oxidation state, and (c) the electrical resistivity ρ at 323 K on the value of x for $Ca_{0.9-x}Sr_xYb_{0.1}MnO_{3-\delta}$ (x=0, 0.025, 0.05, 0.1, and 0.2).

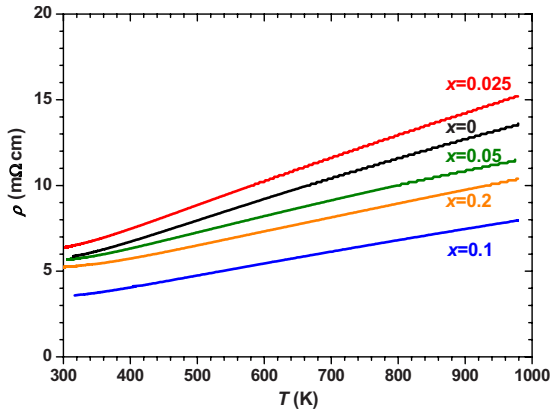

FIG. 4. (Color online) The temperature dependence of the electrical resistivity ρ for $Ca_{0.9-x}Sr_xYb_{0.1}MnO_{3-\delta}$ (x=0, 0.025, 0.05, 0.1, and 0.2).

a, b, c, and V roughly increase with increasing Sr doping, mainly as a result of the difference between the ionic radius[22] of Ca^{2+} (0.134 nm) and that of Sr^{2+} (0.144 nm). The relationship of the lattice parameters a, b, and $c/\sqrt{2}$ can provide a measure of the distortion of the unit cell.[23] Generally, two types of orthorhombic structure can be distinguished. The O-type orthorhombic structure, which is characterized by the relationship $a \leq c/\sqrt{2} \leq b$, exists when the degree of lattice deformation is relatively small, whereas the O'-type orthorhombic structure, with $c/\sqrt{2} \leq a \leq b$, exists in the case of enhanced lattice deformation. In this study, the structure of the $Ca_{0.9-x}Sr_xYb_{0.1}MnO_{3-\delta}$ was of the O-type in the composition range $0 \leq x \leq 0.2$.

The results of chemical composition analysis are summarized in Table I. The cationic compositions of Sr, Yb, and Mn agreed well with the theoretical values, whereas those of Ca deviated slightly from the corresponding stoichiometric compositions, particularly for the compositions in which $x=0$ or $x=0.025$. The reason for this deviation in the composition of Ca is still unclear, but a departure from the intended mixture composition is a possibility. There is also an oxygen deficiency of $0.01 \leq \delta \leq 0.12$ for $Ca_{0.9-x}Sr_xYb_{0.1}MnO_{3-\delta}$ ($0 \leq x \leq 0.2$), as previously reported for other electron-doped calcium manganites.[24,25] The Mn oxidation state, shown in Fig. 3(b), was calculated from the formal charge and the measured chemical compositions for each element. From the calculated Mn oxidation state, it is obvious that Mn^{3+} and Mn^{4+} ions coexist in all the samples, and free electrons are presumed to be generated to a greater degree in the compound with the lower Mn oxidation state. Thus, the relative concentration of carriers in these samples can be evaluated indirectly from the oxidation state of Mn. The differences in the oxidation state of Mn arise from deviations in the cationic compositions and from oxygen deficiencies. The experimental bulk density for all the samples, which was independent of the sample composition, was ~73% of the theoretical density, indicating that the effect of the bulk density on ρ and κ is almost negligible (Table II).

The electrical properties of electron-doped manganites, $(M_{1-x}Ca_x)MnO_3$ (M=La, Nd, or Gd), have been previously investigated in detail.[25–27] According to the reports of these studies, the electrical resistivity of electron-doped manganites exhibits n-type semiconducting behavior below room temperature, and the transport properties could be well interpreted in the framework of variable-range hopping of electrons. At high temperatures, a metal–insulator transition occurs as a result of a change in the spin state of Mn^{3+} and then the value of ρ increases with increasing temperature. The temperature dependence of ρ for the $Ca_{0.9-x}Sr_xYb_{0.1}MnO_{3-\delta}$ is shown in Fig. 4. The ρ values for all samples were in the range 3–16 mΩ cm over the entire temperature range examined, and they increased with increasing temperature, indicating a metallic behavior. This is a similar behavior to that of the electron-doped manganites above the metal-insulator transition temperature.[28] Thus, the metallic conduction can be attributed to the delocalized character of e_g electrons, which are derived from the partial t_{2g} electrons of the Mn^{3+} ion above the metal-insulator transition. Generally the ρ value for calcium manganites is governed by the effective e_g bandwidth, W, which, in turn, is determined by the degree of the hybridization between the Mn $3d$ e_g and O $2p\sigma$ states.[29]

TABLE II. Bulk densities of $Ca_{0.9-x}Sr_xYb_{0.1}MnO_{3-\delta}$ (x=0, 0.025, 0.05, 0.1, and 0.2).

x		0	0.025	0.05	0.1	0.2
Theoretical bulk density (d_t)	g cm^{-3}	4.99	5.02	5.04	5.11	5.22
Experimental bulk density (d_e)	g cm^{-3}	3.63	3.64	3.66	3.80	3.79
	%TD[a]	73	73	73	74	73

[a]%TD=Percentage of theoretical bulk density.

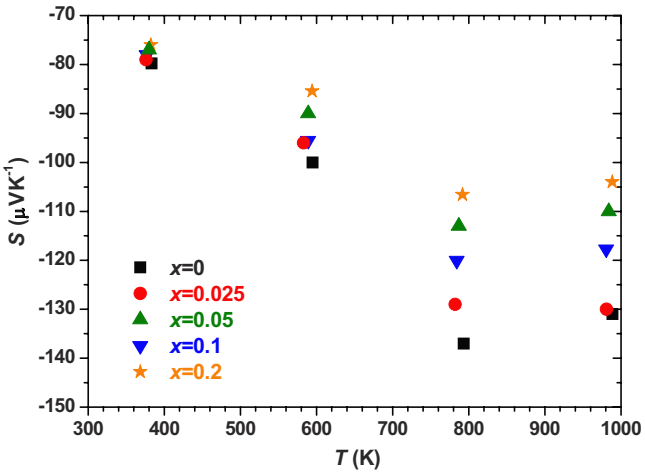

FIG. 5. (Color online) The temperature dependence of the Seebeck coefficient S for $Ca_{0.9-x}Sr_xYb_{0.1}MnO_{3-\delta}$ (x=0, 0.025, 0.05, 0.1, and 0.2).

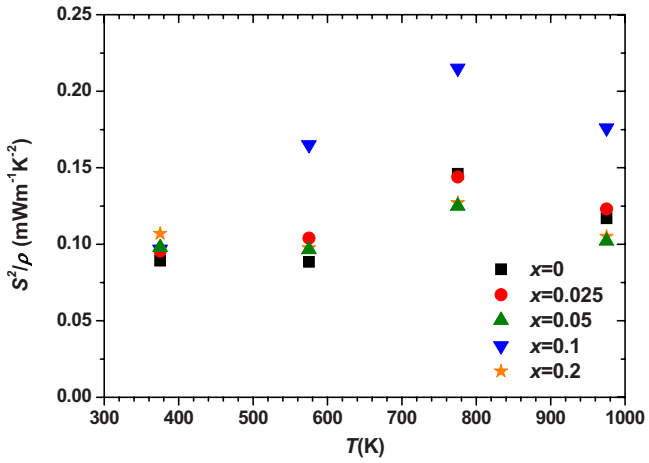

FIG. 6. (Color online) The temperature dependence of the power factor S^2/ρ for $Ca_{0.9-x}Sr_xYb_{0.1}MnO_{3-\delta}$ (x=0, 0.025, 0.05, 0.1, and 0.2).

The magnitude of W is controlled by changes in the tolerance factor, as calculated by Eq. (2); this is a relevant parameter for estimating the magnitude of distortion in ABO_3-type perovskite structures and is defined as follows:[30]

$$t = (r_A + r_O)/\sqrt{2}(r_B + r_O), \tag{2}$$

where r_A, r_B, and r_O represents the ionic radii of A-site, B-site, and oxide ions, respectively. In this study, ionic radii of sixfold coordination for r_A of Shannon[22] were used for 12-coordination of the A-site cations because no complete list of values for 12-coordination of all the elements exists. From Figs. 3(a)–3(c), we can see that the larger is the value of t, the smaller is that of ρ at 323 K. Generally with increasing t, the distortion of the MnO_6 octahedron decreases, corresponding to a decrease in bending of the Mn–O–Mn bond; this decreased bending widens the bandwidth of the conduction band, leading to an increase in the mobility of e_g electrons and a consequent decrease in the value of ρ. At the same time, we believe that distortion of the MnO_6 octahedron also affects the oxidation state of Mn. As reported by Taguchi *et al.*,[31] the amount of oxygen deficiency increases with increasing temperature, and the symmetry of the crystal structure also increases with increasing oxygen deficiency in $CaMnO_{3-\delta}$. It is not, therefore, surprising that the symmetry of the crystal structure is closely related to the level of oxygen deficiency. In this study, we found that when a sample of calcium manganite has a less-distorted crystal structure (high t), the average Mn oxidation state tends to be lower, as shown in Figs. 3(a) and 3(b). This suggests that an increase in the average ionic radius of cation sites will induce an oxygen deficiency in order to permit stabilization of the crystal structure; the deviation of the oxygen content from the stoichiometric value changes with the ratio of Mn^{4+} to Mn^{3+}, resulting in a variation in the concentration of carriers in $Ca_{0.9-x}Sr_xYb_{0.1}MnO_{3-\delta}$. We therefore conclude that distortion of the MnO_6 octahedron could strongly affect both the electron mobility and the concentration of carriers in $Ca_{0.9-x}Sr_xYb_{0.1}MnO_{3-\delta}$ ($0 \le x \le 0.2$). The temperature dependence of S is shown in Fig. 5. The S values for all the samples are negative, showing that the predominant carriers are electrons over the entire temperature range examined. The absolute value of S at room temperature varied from -80 to -70 μV K^{-1}, and that at 973 K varied from -140 to -100 μV K^{-1}. These values are similar to other reported values for electron-doped calcium manganites.[14,15] It has been reported that, although structural distortions can observably affect the electronic conductivity, they have less effect on S,[14,15] so the average Mn oxidation state is the main factor that determines the value of S. In this study, however, the magnitude of the S cannot be explained simply in terms of the oxidation state of Mn. This suggests that band structural modifications, which are related to changes in the overlap of the atomic orbitals of Mn and O induced by structural distortions, also affect the value of S in these samples. The temperature dependence of the power factor S^2/ρ is shown in Fig. 6. For all the samples, S^2/ρ reached a maximum value at 773 K and then decreased slightly. The highest value of S^2/ρ at 773 K (0.22 mW m^{-1} K^{-2}) was obtained with $Ca_{0.8}Sr_{0.1}Yb_{0.1}MnO_{3-\delta}$ as a result of its low ρ value combined with its moderate S value.

The temperature dependence of κ is shown in Fig. 7. To examine the values of κ for our samples in more detail, the

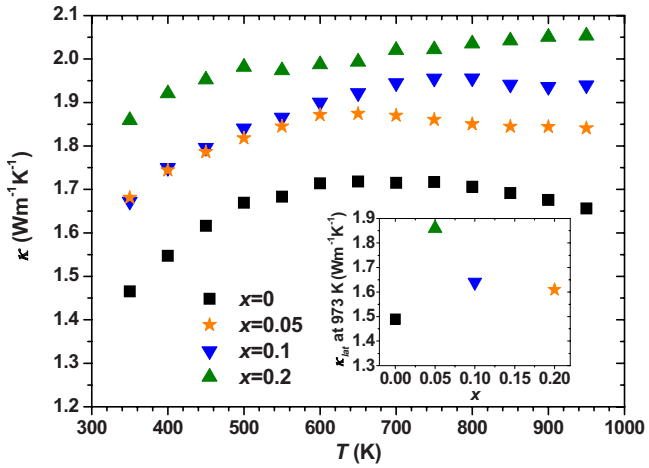

FIG. 7. (Color online) The temperature dependence of the thermal conductivity κ for $Ca_{0.9-x}Sr_xYb_{0.1}MnO_{3-\delta}$ (x=0, 0.05, 0.1, and 0.2). The inset shows a plot of the lattice thermal conductivity κ_{lat} at 973 K vs x.

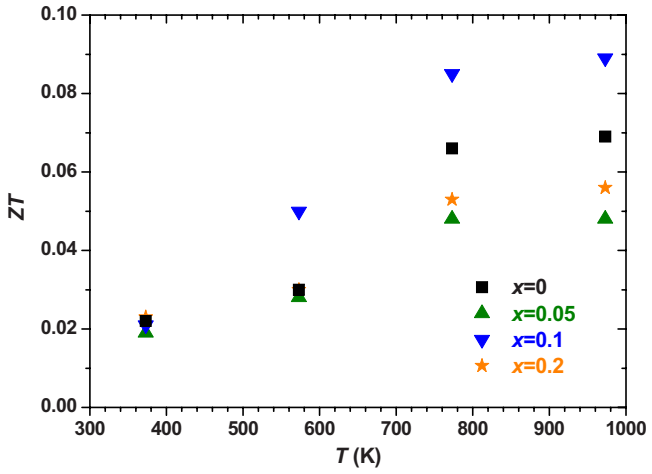

FIG. 8. (Color online) The temperature dependence of the dimensionless figure of merit ZT for $Ca_{0.9-x}Sr_xYb_{0.1}MnO_{3-\delta}$ (x=0, 0.05, 0.1, and 0.2).

lattice contribution κ_{lat} was estimated by means the equation below. It is well known that the total thermal conductivity κ_{total} of solids can be written as follows:

$$\kappa_{total} = \kappa_{lat} + \kappa_{el}, \tag{3}$$

where κ_{lat} is the lattice contribution and κ_{el} is the electronic contribution. κ_{el} can be calculated by using the Wiedemann–Franz–Lorenz relationship,

$$\kappa_{el} = L\sigma T, \tag{4}$$

where L is the Lorenz number and T is the absolute temperature. κ_{lat} is then obtained by subtracting κ_{el} from κ_{total}. The lattice contributions κ_{lat} at room temperature are shown in the inset of Fig. 7. For all samples, the contribution from phonons is more important than that from electrons. Because the radius and mass of Sr^{2+} and Ca^{2+} ions are different, substitution of Sr^{2+} for Ca^{2+} can affect the value of κ_{lat}. Among the samples with $0 \leq x \leq 0.2$, the value of κ_{lat} for $x=0$ has the lowest value of about 1.49 W m^{-1} K^{-1}. For $x \geq 0.05$, the value of κ_{lat} tends to decrease slightly with increasing Sr concentration. One possible explanation of this behavior is that both the crystal distortion and the mass difference between Ca^{2+} and Sr^{2+} contribute to κ_{lat}. Because the sample with $x=0$ has the lowest value of t, the strong crystal distortion induces enhanced phonon scattering, resulting in the lowest κ_{lat} value among all the samples. On the other hand, for $x \geq 0.05$, because the difference in crystal distortion is relatively small, the mass difference between Ca^{2+} and Sr^{2+} is the dominant factor in controlling the value of κ_{lat}, which means that with increasing Sr substitution, κ_{lat} gradually decreases from ~1.86 to 1.61 W m^{-1} K^{-1}.

The temperature dependence of the value of ZT is shown in Fig. 8. The ZT value for all the samples increased with increasing temperature over the whole temperature range examined. The maximum ZT value of 0.09 at 973 K was obtained for the composition with $x=0.1$; this value was about 30% higher than that of a sample with no Sr doping. Thus, the sample with the composition $x=0.1$ has the highest ZT value because of its low ρ value, induced by decreased crystal distortion, combined with its moderate values of S and κ.

This study showed that control of crystal distortion is a key factor in enhancing the thermoelectric properties of electron-doped calcium manganites. Fortunately, this system is so structurally flexible that both A and B sites can be substituted by a variety of elements. This means that numerous variations on crystal distortion are possible in this system. Furthermore, some calcium manganites are known to exist as electronically phase-separated nanometer-scale mixtures of two phases at very low temperatures; this is believed to be essential to the fascinating phenomenon of colossal magnetoresistivity.[32,33] This type of nanophase separation can be regarded as a spatial inhomogeneity of the crystal distortion at the nanometer scale. The fabrication of materials showing similar nanophase separation at the higher temperature where thermoelectric materials can be used is expected to lead to the discovery of new thermoelectric materials with intriguing transport properties.

IV. CONCLUSIONS

The effect of substitution of Ca sites by Sr on the thermoelectric properties of $Ca_{0.9}Yb_{0.1}MnO_{3-\delta}$ (x=0, 0.025, 0.05, 0.1, and 0.2) was investigated in an attempt to improve the thermoelectric performance of the material. All the samples consisted of a single phase with an orthorhombic structure. The values of a, b, c, and V tended to increase with increasing Sr doping, mainly as a result of the difference between the ionic radius of Ca^{2+} and that of Sr^{2+}. The cationic compositions deviated slightly from the corresponding stoichiometric compositions, especially for the compositions where $x=0$ or 0.025; there was also oxygen deficiency of $0.01 \leq \delta \leq 0.12$ in $Ca_{0.9-x}Sr_xYb_{0.1}MnO_{3-\delta}$ ($0 \leq x \leq 0.2$). The ρ values for all the samples was strongly affected by distortion of the MnO_6 octahedron, which had a marked effect on both the electron mobility and carrier concentration in $Ca_{0.9-x}Sr_xYb_{0.1}MnO_{3-\delta}$ ($0 \leq x \leq 0.2$). For all the samples, the S value was not governed simply by the carrier concentration, which is a different result to those previously reported and indicates that band structural modifications, which are correlated with changes in the overlap of the atomic orbitals of Mn and O induced by structural distortion, also affect the value of S in these samples. The values of κ for all samples were governed mainly by the value of κ_{lat}, which, in turn, was affected by both the crystal distortion and the difference in mass between Ca^{2+} and Sr^{2+}. The highest value of ZT of 0.09 at 973 K was achieved with the sample with $x=0.1$; this is due to the low ρ of this sample combined with its moderate values of S and κ.

ACKNOWLEDGMENTS

A part of this work was supported by a grant-in-aid for scientific research from the Japan Society for the Promotion of Science.

[1] *CRC Handbook of Thermoelectrics*, edited by D. M. Rowe (CRC Press, New York, 1995).
[2] T. M. Tritt, Science **283**, 804 (1999).
[3] B. C. Sales, D. Mandrus, and R. K. Williams, Science **272**, 1325 (1996).
[4] D.-Y. Chung, T. Hogan, P. Brazis, M. R. Lane, C. Kamewurf, M. Bastea, C. Uher, and M. G. Kanatzidis, Science **287**, 1024 (2000).

[5]T. Caillat, J.-P. Fleurial, and A. Borshchevsky, J. Phys. Chem. Solids **58**, 1119 (1997).
[6]I. Terasaki, Y. Sasago, and K. Uchinokura, Phys. Rev. B **56**, R12685 (1997).
[7]R. Funahashi, I. Matsubara, H. Ikuta, T. Takeuchi, U. Mizutani, and S. Sodeoka, Jpn. J. Appl. Phys., Part 2 **39**, L1127 (2000).
[8]R. Funahashi and I. Matsubara, Appl. Phys. Lett. **79**, 362 (2001).
[9]S. Ohta, T. Nomura, H. Ohta, and K. Koumoto, J. Appl. Phys. **97**, 034106 (2005).
[10]M. Ohtaki, T. Tsubota, K. Eguchi, and H. Arai, J. Appl. Phys. **79**, 1816 (1996).
[11]A. Maignan, C. Michel, M. Hervieu, and B. Raveau, Solid State Commun. **101**, 277 (1997).
[12]C. R. Wiebe and J. E. Greedan, Phys. Rev. B **64**, 064421 (2001).
[13]M. Ohtaki, H. Koga, T. Tokunaga, K. Eguchi, and H. Arai, J. Solid State Chem. **120**, 105 (1995).
[14]D. Flahaut, T. Mihara, R. Funahashi, N. Nabeshima, K. Lee, H. Ohta, and K. Koumoto, J. Appl. Phys. **100**, 084911 (2006).
[15]Y. Wang, Y. Sui, and W. Su, J. Appl. Phys. **104**, 093703 (2008).
[16]G. Xu, R. Funahashi, Q. Pu, B. Liu, R. Tao, G. Wang, and Z. Ding, Solid State Ionics **171**, 147 (2004).
[17]L. Bocher, M. H. Aguirre, D. Logvinovich, A. Shkabko, R. Robert, M. Trottmann, and A. Weidenkaff, Inorg. Chem. **47**, 8077 (2008).
[18]S. Urata, R. Funahashi, T. Mihara, A. Kosuga, S. Sodeoka, and T. Tanaka, Int. J. Appl. Ceram. Technol. **4**, 535 (2007).
[19]A. Kosuga, S. Urata, K. Kurosaki, S. Yamanaka, and R. Funahashi, Jpn. J. Appl. Phys. **47**, 6399 (2008).
[20]K. R. Poeppelmeier, M. E. Leonowicz, J. C. Scanlon, J. M. Longo, and W. B. Yelon, J. Solid State Chem. **45**, 71 (1982).
[21]K. Kuroda, N. Ishizawa, N. Mizutani, and M. Kato, J. Solid State Chem. **38**, 297 (1981).
[22]R. D. Shannon, Acta Crystallogr., Sect. A: Cryst. Phys., Diffr., Theor. Gen. Crystallogr. **32**, 751 (1976).
[23]G. Ch. Kostogloudis, P. Fertis, and Ch. Ftikos, Solid State Ionics **118**, 241 (1999).
[24]P. X. Thao, T. Tsuji, M. Hashida, and Y. Yamashita, J. Ceram. Soc. Jpn. **111**, 544 (2003).
[25]H. Taguchi and M. Nagao, J. Solid State Chem. **82**, 8 (1989).
[26]H. Taguchi and M. Shimada, J. Solid State Chem. **63**, 290 (1986).
[27]H. Taguchi, M. Nagao, and M. Shimada, J. Solid State Chem. **76**, 284 (1988).
[28]T. Kobayashi, H. Takizawa, T. Endo, T. Sano, and M. Shimada, J. Solid State Chem. **92**, 116 (1991).
[29]S. Mollah, H. L. Huang, H. D. Yang, S. Pal, S. Taran, and B. K. Chaudhuri, J. Magn. Magn. Mater. **284**, 383 (2004).
[30]V. M. Goldschmidt, *Geochemische Verteilungsgesetze der Elemente*, (Skrifter Norske Videnskaps-Akademii, Oslo, I. Mat.-Naturv Klasse l, 1926).
[31]H. Taguchi, N. Nagao, T. Sato, and M. Shimada, J. Solid State Chem. **78**, 312 (1989).
[32]M. Uehara, S. Mori, C. H. Chen, and S.-W. Cheong, Nature (London) **399**, 560 (1999).
[33]R. Mathieu, and Y. Tokura, J. Phys. Soc. Jpn. **76**, 124706 (2007).